nature structural & molecular biology

SUPPLEMENTARY INFORMATION

https://doi.org/10.1038/s41594-018-0057-1

In the format provided by the authors and unedited.

Mapping interactions with the chaperone network reveals factors that protect against tau aggregation

Sue-Ann Mok[1], Carlo Condello[1], Rebecca Freilich[2], Anne Gillies[2], Taylor Arhar[2], Javier Oroz[3], Harindranath Kadavath[3], Olivier Julien[2], Victoria A. Assimon[2], Jennifer N. Rauch[2], Bryan M. Dunyak[2], Jungsoon Lee[4], Francis T. F. Tsai[4], Mark R. Wilson[5], Markus Zweckstetter[3,6,7], Chad A. Dickey[8] and Jason E. Gestwicki[1,2*]

[1]Department of Neurology, University of California at San Francisco, San Francisco, CA, USA. [2]Department of Pharmaceutical Chemistry, University of California at San Francisco, San Francisco, CA, USA. [3]Deutsches Zentrum für Neurodegenerative Erkrankungen (DZNE), Göttingen, Germany. [4]Department of Biochemistry and Molecular Biology, Baylor College of Medicine, Houston, TX, USA. [5]Ilawarra Health and Medical Research Institute, School of Biological Sciences, University of Wollongong, Wollongong, New South Wales, Australia. [6]Max-Planck-Institut für Biophysikalische Chemie, Goettingen, Germany. [7]Department of Neurology, University Medical Center Göttingen, University of Göttingen, Göttingen, Germany. [8]Department of Molecular Medicine and Byrd Alzheimer's Research Institute, University of South Florida, Tampa, FL, USA. Deceased: Chad A. Dickey. *e-mail: jason.gestwicki@ucsf.edu

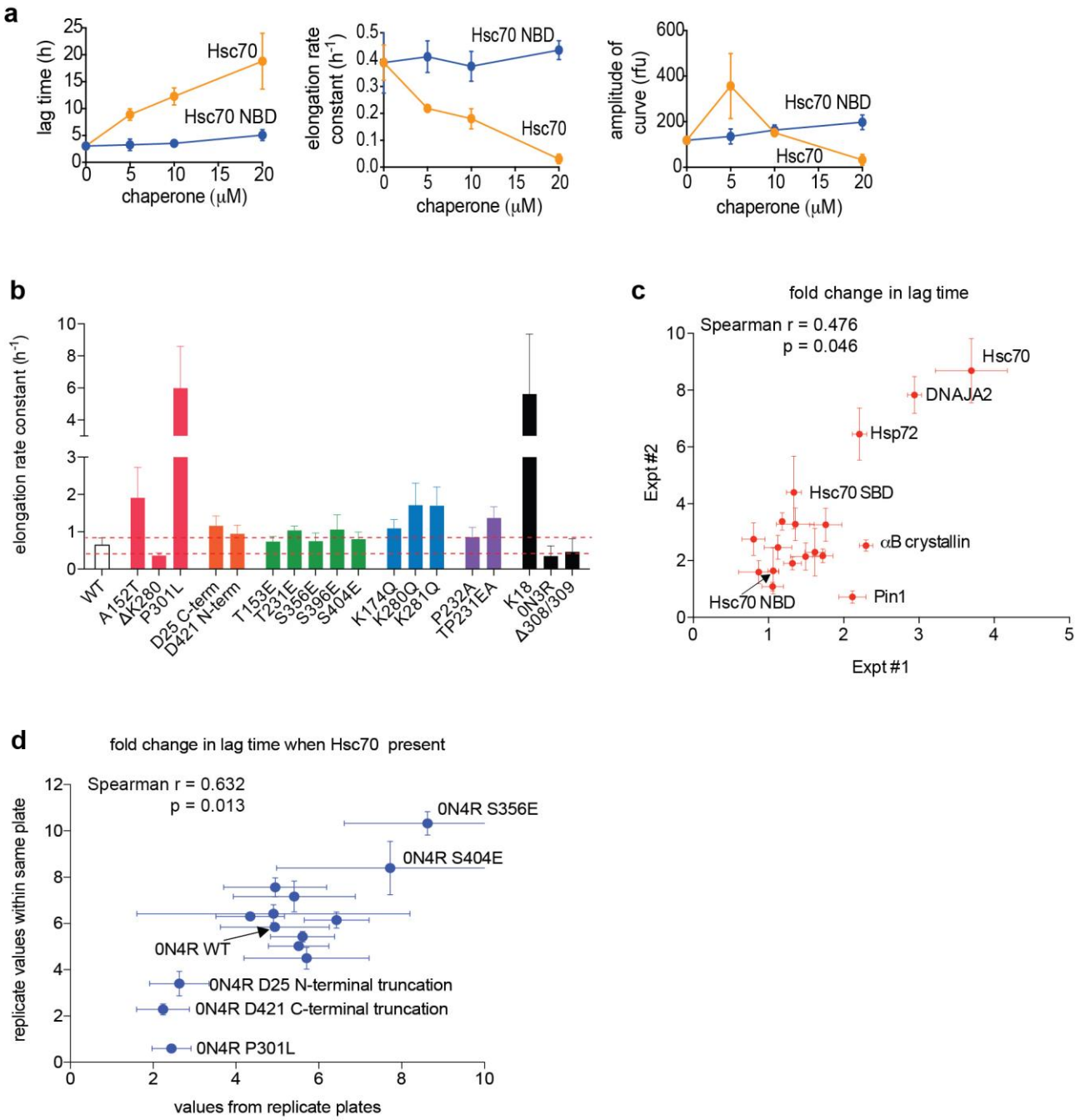

Supplementary Figure 1

Supporting data for in vitro tau aggregation screen

a) Addition of Hsc70 to tau prior to aggregation induction leads to dose-dependent effects on aggregation. 0N4R tau^{WT} incubated with indicated concentrations of Hsc70 or Hsc70$_{NBD}$ was induced to aggregate with the addition of heparin. The aggregation kinetic parameters (lag time, elongation rate constant, and amplitude) calculated from the corresponding ThT aggregation curves are plotted (mean ± SD, triplicates, representative of 3 independent experiments). b) Calculated elongation rate constant for tau variants tested in the *in vitro* aggregation screen (mean ± SD, triplicates). c and d) Replicate experiments demonstrating reproducibility of lag time effects. c) 18 chaperones were assayed for effects on 0N4R tau^{WT} aggregation for two independent experiments. The fold change in lag time due to addition of chaperone was plotted for each experiment on the x and y axes, respectively (mean ± SD, triplicates for each experiment). The calculated values for the Spearman's rank correlation are shown. d) Hsc70 was assayed against the entire panel of 0N4R tau variants in triplicate within the same plate for 3 independent experiments. The fold change in lag time due to addition of full-

length Hsc70 was plotted for each replicate paradigm on the x and y axes, respectively (mean ± SD). The calculated values for the Spearman's rank correlation are shown.

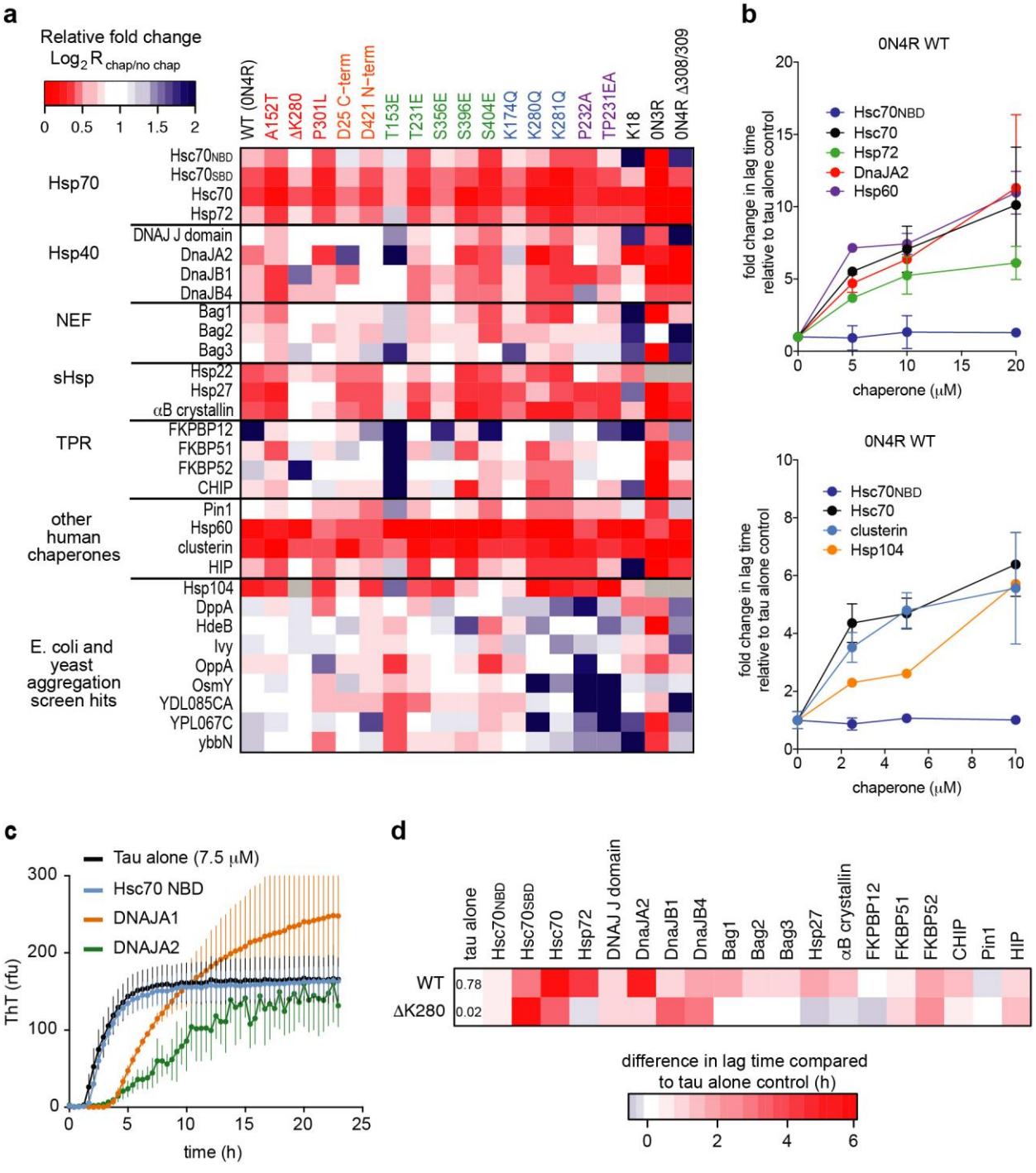

Supplementary Figure 2

Data analysis of additional calculated kinetic parameters from tau aggregation screen

a) Heatmap representing the effect of individual chaperones on the elongation rate constant parameter of aggregation for each tau variant. For each chaperone-tau combination, the $\log_2$ fold change in elongation rate of tau when aggregated in the absence or presence of an equimolar concentration of chaperone was plotted. Red and blue represent chaperone–dependent decreases or increases in aggregation elongation rate constant, respectively. Grey = not tested. b) Dose-dependent effects of chaperone screen hits on tau aggregation lag time. Fold change in lag time of 0N4R tau^{WT} (10 μM) in the presence of multiple chaperone concentrations are plotted (mean ± SD, triplicates). c) Comparison of DnaJA1 and DnaJA2 effects on tau aggregation kinetics. 0N4R tau^{WT} (7.5 μM) was

aggregated in the presence of an equimolar concentration of DnaJA1 or DnaJA2. The ThT fluorescence for each reaction is plotted (mean ± SD from triplicate wells is plotted, representative of 2 independent experiments). d) Heatmap of absolute values for lag time kinetic parameter for 0N4R tau^{WT} and ΔK280 in the presence of chaperones. The calculated lag time (h) is displayed according to the indicated color scale for each chaperone-tau combination (1:1 stoichiometry). The lag time value (h) for each tau variant without chaperone is included.

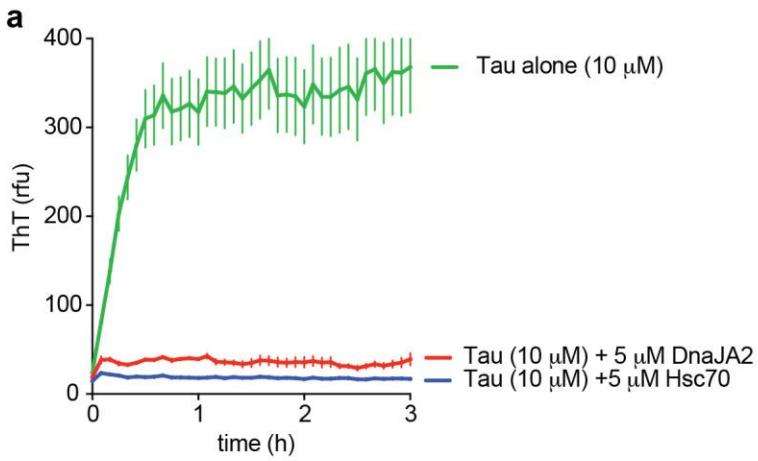

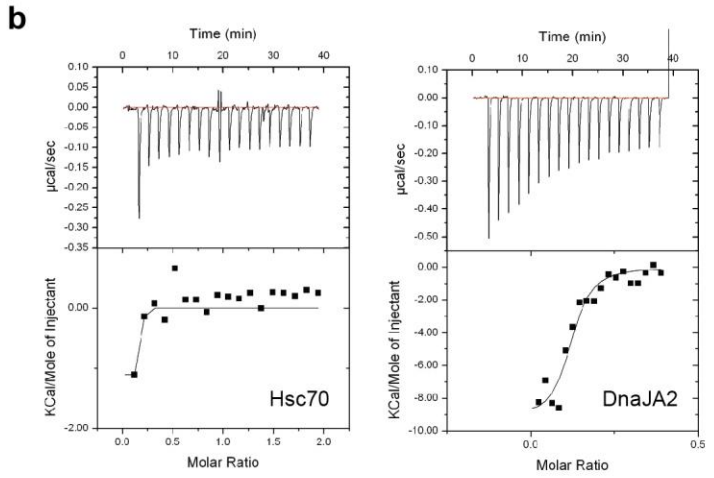

Chaperone	Kd (μM)	N
Hsc70	No binding	No binding
DnaJA2	1.9 ±1.5	0.10±0.03

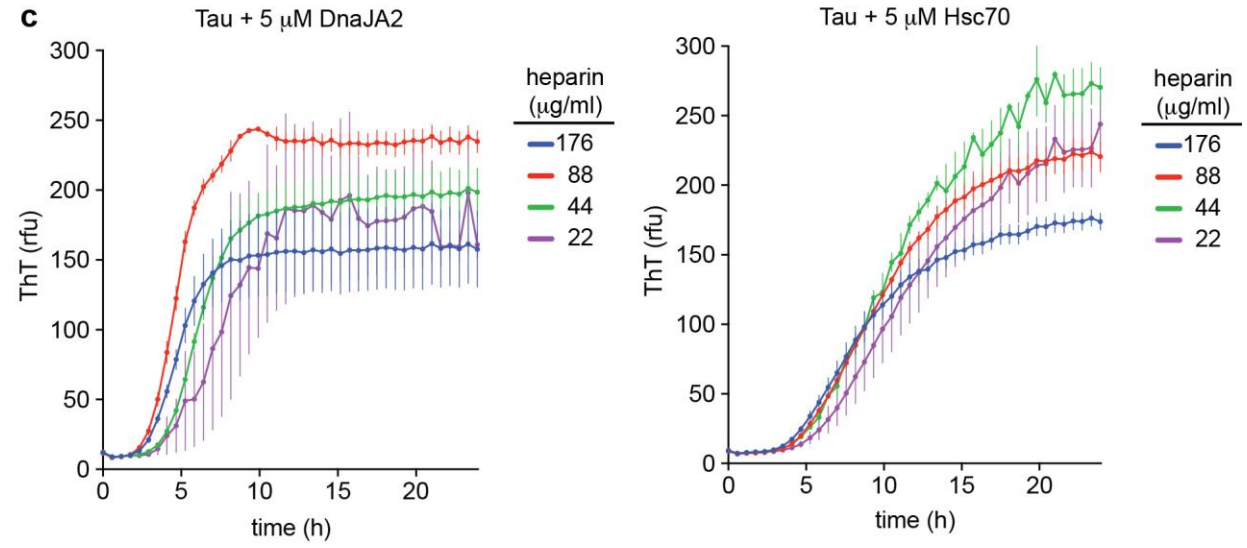

Supplementary Figure 3

DnaJA2 and Hsc70 present similar anti-aggregation behaviors when heparin concentrations are varied or the alternate tau accelerant arachadonic acid is employed

a) 0N4R tau^{WT} (10 μM) was induced with arachadonic acid in the absence or presence of 5 μM Hsc70 or DnaJA2. Thioflavin T fluorescence was used to monitor the aggregation process (mean ± SD from triplicate wells is plotted). b) ITC traces of heparin (200 μM/1mM) titrated into cells containing 100 μM Hsc70 or DnaJA2. The average calculated K_d from duplicate experiments is indicated. c) Example aggregation curves of 0N4R tau^{WT} (10 μM) induced with a range of concentrations of heparin in the presence of 5 μM Hsc70 or DnaJA2 (mean ± SD, triplicates).

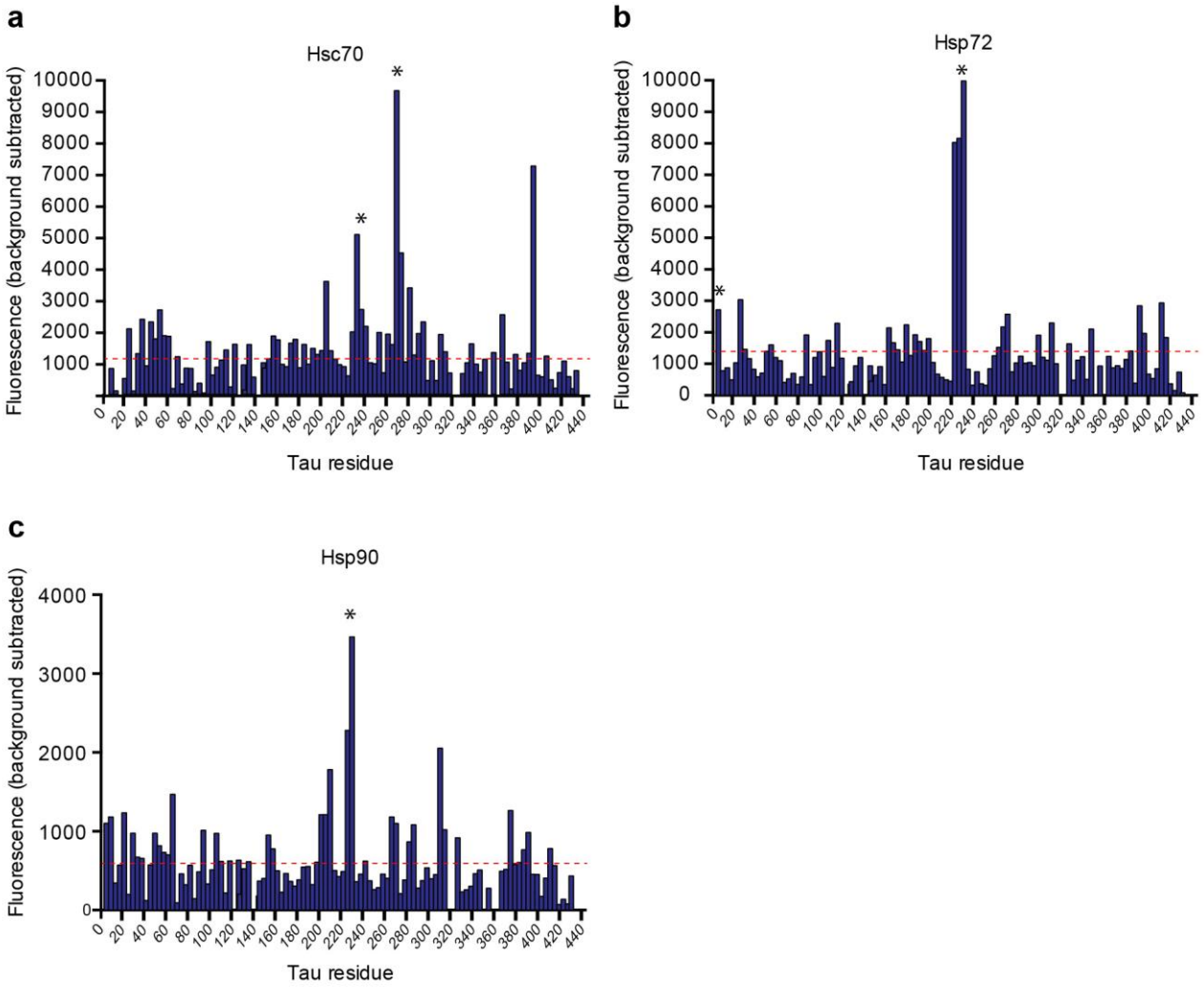

Supplementary Figure 4

Representative data of Hsc70, Hsp72 and Hsp90 binding to the tau peptide array from three independent experiments

Raw signal intensity (rfu) of chaperone binding as assayed via fluorescently-tagged His-antibody is plotted for each peptide. The N-terminal amino acid is used to mark the position of each peptide within the 2N4R tau sequence. Dotted red line for each plot represents the mean of the corresponding array dataset. False positive peptide values in the array are not graphed for clarity. Bound peptide regions as defined in materials and methods are indicated by (*).

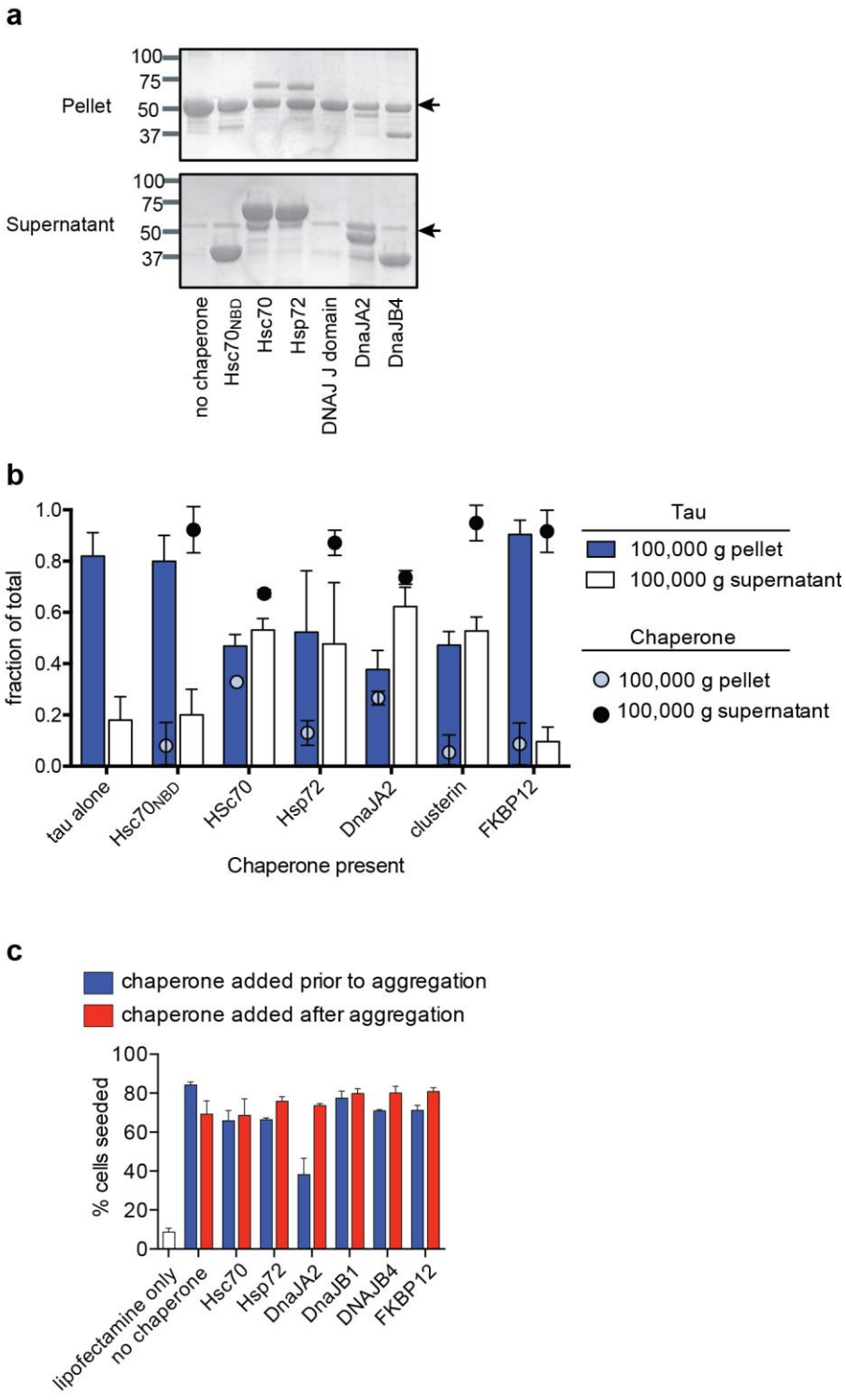

Supplementary Figure 5

Chaperone screen hits present during the aggregation of tau reduce the amount of pelletable tau material

a) SDS-PAGE of pellet and supernatant fractions from tau aggregation samples. 10 μM tau samples aggregated for 24h in the presence of indicated chaperones (20 μM) were centrifuged at 100,000 g for 1 h and equal fractions of reactions were subject to SDS-PAGE. b) Quantification of bands corresponding to tau (bars) and indicated chaperone (circles) for each aggregated tau sample is plotted as the fraction of the total amount present in the supernatant plus pellet (mean ± SEM from 3 independent experiments). c)

Chaperone addition to pre-formed tau fibrils does not alter their ability to seed aggregation in clone 1 cells. Samples of 0N4R tau^{WT} (10 μM) aggregated in the presence of indicated chaperones (20 μM) were compared to samples of 0N4R tau^{WT} fibrils formed without chaperones followed by incubation with 20 μM of chaperone for 1 h. Equal amounts of tau from each sample (blue, chaperone added prior to aggregation, red, chaperone added after aggregation) were transfected into clone 1 cells and the percentage of cells that formed punctae are plotted (mean± SD, triplicates).

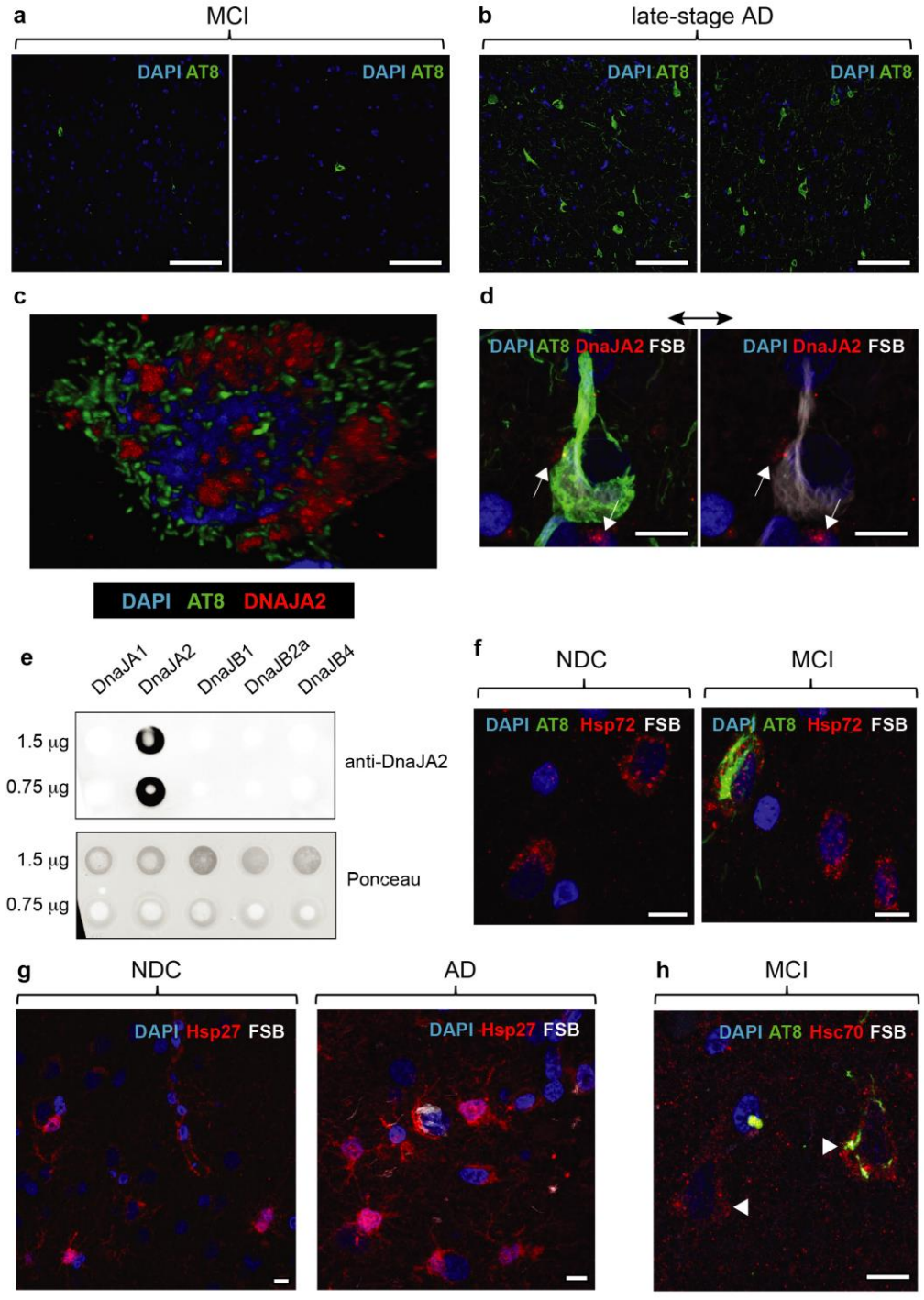

Supplementary Figure 6

Immunostaining of DnaJA2 and other chaperones in samples from patients with MCI and AD

Fixed brain sections from MCI, late-stage AD, or non-demented control (NDC) samples were co-stained for chaperone (red), phospho-tau (AT8, green) antibodies as well as the amyloid-binding small molecule, FSB (white). Nuclei were visualized with propidium iodide (PI) stain. a and b) Low magnification images show that MCI samples have a low incidence of AT8 positive neurons compared to late-stage AD samples. Scale bar = 100 microns**.** c) In an MCI sample, 3D rendering of one face of a neuron showing DnaJA2 is interspersed between or surrounds areas of AT8 staining. Colocalization between DnaJA2 and AT8 is not evident. The neuron shown is the same as presented in Fig 5b (main text). d) Representative image from late-stage AD samples showing increased DnaJA2 staining adjacent (arrows), but not within, an AT8 and FSB positive neuron. Scale bar = 10 microns. e) DnaJA2 antibody does not detect other J-proteins such as the closely related family member, DnaJA1. Dot blot of recombinant chaperones with the same DnaJA2 antibody used for immunostaining. Ponceau stain of the same blot to verify protein transfer to membrane (representative of 2 independent experiments). f-h) Representative images of chaperone staining patterns in MCI and non-demented control samples. Scale bar = 10 microns for all images. Samples probed with antibodies against f) Hsp72, g) Hsp27 and h) Hsc70. Arrowheads mark neurons in h). Note that sections stained for Hsp27 could not be co-stained for phospho-tau (AT8).

Supp. Table 1. References for mutations and post-translational modifications in tau mimicked in this study

Variant	Mutation or PTM category	Primary or review reference
A152T	mutation	[65]
N279K	mutation	[60]
ΔK280	mutation	[60]
P301L	mutation	[60]
P301S	mutation	[60]
K317M	mutation	[60]
R406W	mutation	[60]
T153E	phosphorylation	[66]
T231E	phosphorylation	[66]
S356E	phosphorylation	[66]
S396E	phosphorylation	[66]
S404E	phosphorylation	[66]
K174Q	acetylation	[67]
K280Q	acetylation	[68]
K281Q	acetylation	[68]
D25 cleavage	caspase cleavage	[69]
D421 cleavage	caspase cleavage	[61]

Supp. Table 2. Properties of high frequency-bound tau peptides within the microarray. Biochemical properties of each peptide were determined using the ExPASy ProtParam tool. Amino acids corresponding to PHF6 and PHF6* aggregation motifs are in highlighted in bold.

peptide #	peptide sequence	pI	instability	aliphatic	GRAVY
5	RQEFEVMEDHAGTYG	4.4	36.5	26	-1.153
9	EVMEDHAGTYGLGDR	4.31	5.83	52	0.88
220	TREPKKVAVVRTPPK	11.1	29.3	64.67	-1.067
224	KKVAVVRTPPKSPSS	11.26	71.49	64.67	-0.647
228	VVRTPPKSPSSAKSR	12	89.99	45.33	-1.02
264	ENLKHQPGGGK**VQII**	8.7	21.65	97.33	-0.72
268	HQPGGGK**VQIINK**KL	10.3	37.43	97.33	-0.747
296	NIKHVPGGGS**VQIVY**	8.6	51.57	110	0.173
300	VPGGGS**VQIVYK**PVD	5.8	25.73	103.33	0.26

Supp. Table 3. References for protein purification methods

Construct	Species	Gene	Vector	References for protein purification
0N4R tau (WT and variants)	*H. Sapiens*	MAPT	pET28	[70], this paper
K18 tau (244-372)	*H. Sapiens*	MAPT	pRK172	[70], this paper
2N4R tau	*H. Sapiens*	MAPT	pNG2	Adopted from [71]
Hsc70 NBD (1-383)	*H. Sapiens*	HSPA8	pMCSG7	[72]
Hsc70 SBD (394-540)	*H. Sapiens*	HSPA8	pMCSG7	[72]
Hsc70	*H. Sapiens*	HSPA8	pMCSG7	[72]
Hsp72	*H. Sapiens*		pMCSG7	[72]
Hsp72 SBD (394-540)	*H. Sapiens*	HSPA1A	pMCSG7	[72]
J domain (2-108)	*E. coli*	DNAJ	pMCSG7	[73]
DnaJA1	*H. Sapiens*	DNAJA1	pET28	[74]
DnaJA2	*H. Sapiens*	DNAJA2	pMCSG7	[74]
DnaJB1	*H. Sapiens*	DNAJB1	pMCSG7	[74]
DnaJB4	*H. Sapiens*	DNAJB4	pMCSG7	[74]
Bag1	*H. Sapiens*	BAG1	pMCSG7	[74]
Bag2	*H. Sapiens*	BAG2	pMCSG7	[74]
Bag3	*H. Sapiens*	BAG3	pMCSG7	[74]
Hsp22	*H. Sapiens*	HSPB8	pET28a	[75]
Hsp27	*H. Sapiens*	HSPB1	pET21	[75]
αB crystallin	*H. Sapiens*	HSPB5	pMCSG7	[76]
FKBP12	*H. Sapiens*	FKBP1A	pMCSG7	[77]
FKBP51	*H. Sapiens*	FKBP5	pET151	[78]
FKBP52	*H. Sapiens*	FKBP4	pET151	[78]
CHIP	*H. Sapiens*	STUB1	pET151	[78]
Pin1	*H. Sapiens*	PIN1	pMCSG7	This paper
Hsp60	*H. Sapiens*	HSPD1	pMCSG7	This paper
Clusterin	*H. Sapiens*	CLU	N/A	[79]
HIP	*H. Sapiens*	ST13	pET28	[80]
Hsp104	*S. cerevisiae*	HSP104	pPROEX HTb	This paper

Supp. Table 4. Primary antibody information for immunoblots and immunostaining

Target	host	dilution	company	catalogue #/clone ID
DnaJA2	Rabbit	1:200	Origene	TA501710/OTI2A2
DnaJB4	Rabbit	1:200	Atlas Antibodies	HPA028383
Hsc70	Rabbit	1:200	Enzo	ADI-SPA-816-F
Hsp27	Mouse	1:200	StressMarq	SMC-161/5D12-A12
Hsp72	Rabbit	1:200	Enzo	ADI-SPA-811
Phospho Ser202/Thr205 Tau (AT8)	Mouse	1:300	Pierce	MN1020/AT8